Metastability in Magnetically Confined Plasmas

B. H. Fong,* S. C. Cowley, and O. A. Hurricane
University of California at Los Angeles, 405 Hilgard Avenue, Los Angeles, California 90095-1547
(Received 11 November 1998)

The parameter space of magnetically confined plasmas near marginal instability for interchange-type modes is divided into three regions according to qualitative stability properties. Region I is linearly stable though nonlinearly unstable to large excitations. Region II is linearly unstable, nonlinearly stable to small excitations, and nonlinearly unstable to large excitations. Region III is linearly and nonlinearly unstable. For an equilibrium evolving through marginal stability, region III and therefore explosive instability are inevitably encountered. [S0031-9007(99)09345-X]

PACS numbers: 52.35.Py, 52.30.Bt, 52.35.Mw, 52.65.Kj

The line-tied interchange and ballooning instabilities play a prominent role in both laboratory and space plasmas. In tokamak and magnetospheric plasmas, pressure-driven modes are thought to account for such explosive events as high-β disruptions [1,2] and substorms [3,4], respectively. Thus, the question of stability, and, in particular, nonlinear stability, is crucial to these systems. Nonlinear stability and dynamics take on a dual significance: because of the limited validity of linear expansions, a determination of linear stability necessarily cannot address the possibility of metastability; also, explosive behavior in previously quiescent or slowly evolving systems can never be described by purely linear modes. In this Letter we consider the nonlinear stability and dynamics of the finite Larmor radius (FLR)–modified ideal magnetohydrodynamic (MHD) ballooning mode [5].

Because real unstable physical systems must have evolved from previously stable states, our investigation of nonlinear ballooning modes centers around the linear marginal stability point. For ideal MHD plasmas, Cowley and Artun found that marginally unstable ballooning modes inevitably evolve towards a finite-time singularity [6]. With lowest order Larmor radius effects included, the finite gyroradius may be sufficient to inhibit the mode's tendency to progress towards finer scales perpendicular to the field line; a nonlinear accessibility condition thus exists, and nonlinear oscillations can arise as linear and nonlinear drives and restoring forces compete. Though the finite Larmor radius term can effectively block access of the mode from linear to nonlinear instability, a region of function space corresponding to unbounded growth nonetheless exists. Indeed, even for linearly stable modes this nonlinearly unstable region still exists. Thus, within the limits of the linear marginal stability assumption, ballooning modes are always metastable and unbounded growth is always possible.

While the analysis to follow applies to more general field configurations, the simple line-tied Rayleigh-Taylor-Parker [7,8] mode provides a more definite physical description of the linear and nonlinear instability processes (Fig. 1). At marginal stability, linear drive and restoring forces—buoyancy and field line bending forces, respectively—nearly cancel, resulting in a small linear growth rate. Nonlinearly, a rising flux tube encounters a positive feedback mechanism: flux tube expansion enforces pressure balance while also resulting in an increase in the linear drive and a decrease in the linear restoring force. The flux tube expansion causes both a decrease in density and a decrease in magnetic field strength due to flux conservation.

By a multiple-scale analysis of the ideal MHD equations incorporating the usual ballooning ordering [5] and the marginal stability condition, two sets of differential equations can be derived that determine the mode's spatial and temporal dependences [6,9]. The first set is the usual fourth-order coupled set of ordinary differential equations [10] giving the dependences of the mode on the field line coordinate (Z). The shape of the local growth rate function, $\Gamma^2(X)$, is also determined from this set. (We consider only two-dimensional equilibria; Y is the equilibrium ignorable coordinate.) The second set is an envelope equation [5] with the usual linear corrections as well as nonlinear terms. Including the lowest order finite Larmor radius effects [11] at this order gives, after rescaling, a nonlinear partial differential equation describing the temporal and fast perpendicular spatial dependences of the envelope near linear marginal stability:

$$\frac{\partial^2 \xi}{\partial t^2} = \left(1 - \frac{x^2}{\Delta^2}\right)\xi - \frac{\partial^2}{\partial x^2}\int u\, dy + \xi \frac{\partial^2}{\partial x^2}\overline{\xi^2} + (\xi^2 - \overline{\xi^2}) + \nu_i^{*2}\frac{\partial^2 \xi}{\partial y^2}. \quad (1)$$

Here $\xi(x, y, t)$ is the scaled plasma displacement in the X (flux function) direction, $\xi \equiv \partial u/\partial y$, x and y are the scaled X and Y coordinates, and the overbar denotes an average over the y coordinate. The rescaling of the equation leaves equilibrium dependence only in Δ and ν_i^*, which measure the scaled characteristic X width of the local growth rate function and size of the ion diamagnetic drift, respectively. The cubic nonlinearity in Eq. (1) arises from the modification of the equilibrium profiles by the

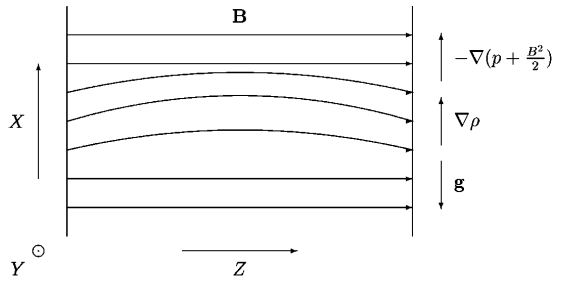

FIG. 1. Equilibrium geometry and perturbed field lines for the Rayleigh-Taylor-Parker mode.

fast compressional wave, resulting in a quasilinear "flattening" of the perturbed profiles; the quadratic, explosive, nonlinearity arises from the positive feedback mechanism described above. Note that the dynamical properties of the equation depend only on Δ, v_i^* and the initial conditions on ξ. (The appearance of Δ results from assuming a parabolic local growth rate profile $[\Gamma^2(X)]$ centered at $x = 0$. Also, the scaled ion diamagnetic drift speed is proportional to Γ_0^{-3}, where Γ_0 is the maximum local linear growth rate; v_i^* therefore decreases as the system moves through the marginal stability boundary. The full expressions for Δ and v_i^* in terms of unnormalized quantities are lengthy and will be given in a future publication [12].) To avoid a complex linear growth rate, the whole equation has been transformed to the frame moving at one-half the ion diamagnetic drift speed, i.e., $v_i^*/2$. A conserved energy can be derived from the equation by multiplying by $\partial\xi/\partial t$ and integrating over the fast perpendicular coordinates and time, yielding

$$E = \int dx\, dy \left[\frac{1}{2}\left(\frac{\partial \xi}{\partial t}\right)^2 - \frac{1}{2}\left(1 - \frac{x^2}{\Delta^2}\right)\xi^2 + \frac{1}{2}\left(\frac{\partial u}{\partial x}\right)^2 + \frac{1}{4}\left(\frac{\partial \overline{\xi^2}}{\partial x}\right)^2 - \frac{1}{3}\,\xi^3 + \frac{v_i^{*2}}{2}\left(\frac{\partial \xi}{\partial y}\right)^2 \right], \qquad (2)$$

which is useful in checking numerical simulations as well as in determining the approximate evolution of the mode via a variational principle.

Before considering the nonlinear and metastable properties of Eq. (1), a description of the linear solution is in order. A simple separation of variables gives the linear modes as

$$\xi_{nk} = A_{nk} e^{[\gamma_{nk} t - (k/2\Delta)x^2]} H_n(\sqrt{k/\Delta}\, x)\cos(ky), \qquad (3)$$

where $\gamma_{nk}^2 = 1 - (2n+1)/(k\Delta) - k^2 v_i^{*2}$ and H_n is the nth Hermite polynomial [6]. Equation (1) allows for a spectrum of modes labeled by wave number k and order n of the Hermite polynomial; the most unstable mode is given by $n = 0$ and $k_{\max} = (2\Delta v_i^{*2})^{-1/3}$, with $\gamma^2(k_{\max}) = 1 - 3(v_i^*/2\Delta)^{2/3}$. The system is globally linearly unstable when $v_i^* \le (2\Delta)3^{-3/2}$. Here the finite Larmor radius effect modifies the mathematical properties in an essential way: the most unstable mode corresponds to a finite wave number instead of $k_{\max} \to \infty$ as in the ideal case.

Equation (1) has been simulated directly using a leapfrog scheme on an adaptive mesh. For small initial disturbances, scanning through the (Δ, v_i^*) parameter space not only reproduces the linear stability boundary given above but also reveals a nonlinear accessibility condition dividing linearly unstable systems into two classes. The results of the parameter space scans are shown in Fig. 2: region I consists of linearly stable, oscillatory systems; region II consists of linearly unstable, nonlinearly oscillatory systems; and region III consists of linearly unstable systems evolving directly to explosive instability. The small initial disturbances of the (Δ, v_i^*) parameter scans, however, do not address the question of metastability. For finite initial disturbances, the simulations show that regions I and II systems also evolve towards explosive instability; they are only metastable. Hence, the boundary between regions II and III should properly be called a nonlinear accessibility boundary rather than a nonlinear stability boundary: all regions are nonlinearly unstable.

While the numerical simulations of Eq. (1) give good quantitative demarcations of stability region boundaries, a better understanding of the nonlinear accessibility condition and metastability properties can be obtained from two analytical methods. When the most unstable mode becomes marginally unstable, a bifurcation analysis can be employed to describe the nonlinear stability properties of Eq. (1). By ordering Eq. (1) in the small parameter $\epsilon^{1/2}$ corresponding to the growth rate of the most unstable mode as well as its amplitude, and taking $\xi(x, y, t)$ to lowest order to be the most unstable eigenmode with the substitution of $A(t)$ for $A_{0,k_{\max}} \exp[\gamma(k_{\max})t]$, the time dependence of the amplitude $A(t)$ can be determined via

$$\frac{\partial^2 A}{\partial t^2} = \gamma^2(k_{\max})A + \lambda(k_{\max})A^3, \qquad (4)$$

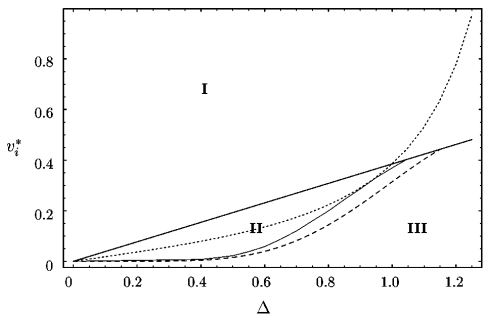

FIG. 2. Portrait of the stability space depending on the parameters Δ and v_i^*. The solid lines are numerical simulation results for linear stability and nonlinear accessibility. The dotted and dashed lines are bifurcation and variational analyses' approximations to the nonlinear accessibility condition. The three regions are discussed in the text.

where $\gamma^2(k_{\max})$ is given above and $\lambda(k_{\max}) \equiv -1/[2\sqrt{2}\,\gamma^2(2k_{\max})] - k_{\max}/(2\sqrt{2}\,\Delta)$. Equation (4), an equation of motion for the amplitude, has an associated anharmonic potential, with the signs of $\gamma^2(k_{\max})$ and $\lambda(k_{\max})$ determining the linear and nonlinear stability properties, respectively, as well as the metastability properties.

From this analysis, a nonlinear stability boundary is given when $\lambda = 0$, i.e., when the quartic part of the potential changes sign. Since the most unstable mode is ordered to have a small growth rate or oscillation frequency, the $2k_{\max}$ mode is still stable, and the first term in $\lambda(k_{\max})$ is positive. This destabilizing first term results from the nonlinear interaction of the fundamental and first harmonic modes, while the stabilizing second term in $\lambda(k_{\max})$ results from the cubic nonlinearity in Eq. (1). Solving for $\lambda > 0$ gives nonlinear instability when $v_i^{*2/3}(5/2 - \Delta^2) < \Delta^{2/3}/2^{1/3}$. Nonlinear instability can be reached either when the diamagnetic drift velocity is sufficiently small (corresponding to a larger Γ_0 and the approach of the first harmonic mode to the linear stability boundary) or the width of the linearly unstable region is sufficiently large. In fact, when $\Delta > \sqrt{5/2}$, the analysis gives nonlinear instability independent of the size of the diamagnetic drift.

From the bifurcation analysis, the stability space is divided into four regions according to the signs of $\gamma^2(k_{\max})$ and λ. The $\lambda = 0$ line is plotted as a dotted line in Fig. 2; we see that the line roughly approximates the computationally determined nonlinear accessibility boundary. The bifurcation analysis, however, gives nonlinear stability when $\lambda < 0$ when, in fact, systems in regions I and II are always nonlinearly metastable. The limitations inherent in the small-amplitude ordering thus prevent a complete consideration of metastability.

To treat the metastability properties at finite amplitude, an approximate variational method is used to determine the dynamics of the system as projected onto the restricted trial function space. Instead of the customary minimization of the potential energy, the action is minimized with respect to the trial function parameters and the equations of motion determined.

The trial function is chosen to satisfy both the linear equation and qualitative nonlinear properties of Eq. (1). Additionally, the trial function must retain the zero y-average properties of the equation [6]. Thus, we choose

$$\xi_{\text{trial}}(A, b, \sigma) = A(t)\exp[-b(t)x^2][1 - \sigma(t)] \times \sum_{m=0}^{\infty} \sigma^m(t)\cos[(m+1)k_{\max}y] \qquad (5)$$

with $|\sigma(t)| < 1$ and $b(t) > 0$. The time dependence of the three parameters will be determined from their respective Euler-Lagrange equations. The trial function can be characterized by its amplitude $A(t)$ as well as its widths in the x and y directions; $\Delta x(t) \equiv [2\sqrt{b(t)}\,]^{-1}$, and $\Delta y(t) \equiv (\pi/k_{\max})[1 - \sigma(t)]/[1 + \sigma(t)]$. Substituting the trial function into Eq. (2) gives the potential and kinetic energies which are used to determine the accessibility condition as well as the equations of motion.

Even within the trial function approximation, the potential energy can be made arbitrarily large and negative regardless of the size of Δ and v_i^*. For large amplitude the potential is dominated by the contributions corresponding to the last three terms in Eq. (2),

$$V \sim A^4 \frac{\Delta y^2}{\Delta x} - A^3 \Delta x\, \Delta y + v_i^{*2} A^2 \frac{\Delta x}{\Delta y}. \qquad (6)$$

The cubic term here causes the mode to grow explosively and to narrow in x and y; the quartic term counters the tendency to narrow in the x direction (and, in fact, forces the mode to spread outwards in the x direction) and slows the growth of the maximum; the FLR term counteracts the narrowing of the mode in the y direction. For large A, choosing Δx and Δy such that $\Delta x^2/\Delta y > A > 1/\Delta y^2$ makes the potential large and negative. The system is thus always metastable: a properly tailored finite initial excitation will result in unbounded growth in all three regions.

For the variational analysis the accessibility condition is derived by solving $V = 0$ in the variationally determined potential energy; assuming the initial mode has zero total energy, the $V = 0$ surface encloses the accessible regions of $(\Delta y, \Delta x, A)$ space. Figures 3 and 4 show the $V = 0$ surfaces in $(\Delta y, \Delta x, A)$ space for (Δ, v_i^*) pairs in regions II and III, respectively. For systems in region II (Fig. 3) a linear instability starting from the lower right of the figure encounters a positive potential barrier that

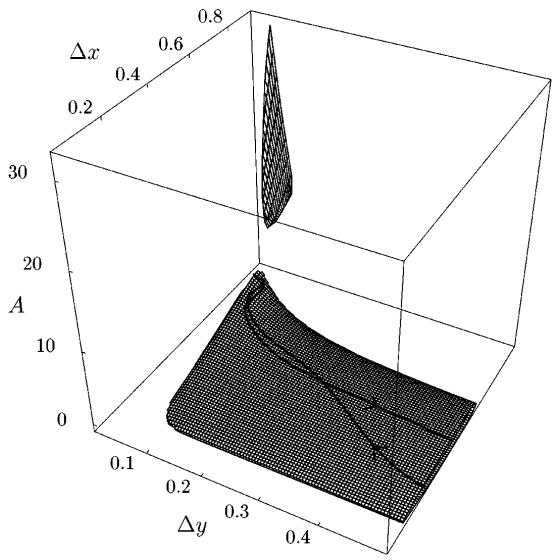

FIG. 3. Zero potential energy surface in $(\Delta y, \Delta x, A)$ space for a variationally determined region II equilibrium. $\Delta = 0.65$, $v_i^* = 0.059$. The trajectory starting from the initial linear instability reaches a finite maximum amplitude and is unable to reach the high amplitude region of negative potential energy.

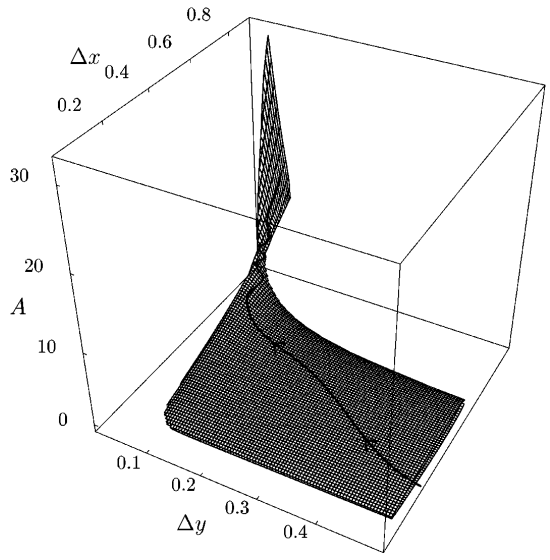

FIG. 4. Zero potential energy surface in $(\Delta y, \Delta x, A)$ space for a region III equilibrium. $\Delta = 0.65, v_i^* = 0.057$. The initial linear instability evolves directly to the region of large amplitude, unbounded growth.

prevents access of the mode to the region of unbounded growth. A linear instability in a region III system (Fig. 4) faces no positive potential barrier and evolves directly to explosive growth. Thus, the variationally determined accessibility condition is the line in (Δ, v_i^*) parameter space that gives precisely a zero potential "barrier" between accessible regions of $(\Delta y, \Delta x, A)$ space; this is plotted as a dashed line in Fig. 2. In determining the possible potential barrier the accessibility condition measures the competition between the explosive and FLR terms in narrowing the y width, and between the cubic and local linear instability drive terms in broadening the x width. The $V = 0$ surface for region I (Δ, v_i^*) pairs looks similar to the region II plot, except that the small-amplitude lower surface is absent.

When unbounded growth ensues whether from region III systems or excited regions I and II systems, the system grows explosively towards a finite-time singularity. In the asymptotic evolution regime, the shape of the instability can be estimated analytically from Eq. (2), yielding $A(t) \sim (t_0 - t)^{-2}$, $\Delta y(t) \sim (t_0 - t)^1$, and $\Delta x(t) \sim (t_0 - t)^{-0.5}$. Numerical integration of the Euler-Lagrange equations derived from the variational method reproduces these scalings close to the singularity time t_0. The full numerical simulation of Eq. (1), however, is unable to evolve sufficiently near the singularity time to reproduce these scalings; the formation of a shock in the x direction eventually exceeds the numerical resolution of the simulation.

For laboratory and space plasmas, systems becoming unstable to the interchange instability must start in region I. As the system evolves through marginal stability, the MHD growth rate Γ_0 increases, the scaled parameter v_i^* decreases (slowly), and Δ remains constant. Thus, as long as Γ_0 increases, the theory predicts that the system eventually reaches the region of nonlinear explosive behavior. In high magnetic field, high β disruptions in the Tokamak Fusion Test Reactor, the change in Γ_0 can be attributed to a fast-growing $n = 1$ kink mode that leads to the steepening of the pressure profile and destabilization of the ballooning mode [1,2,13]. For this case, $\Delta \approx 0.4$–0.6, and taking Γ_0 as evolving on the kink mode's time scale gives approximately 300 μs from linear marginal stability to the explosive singularity, which is roughly the observed time between the onset of the ballooning mode and the disruption. In the case of low field high β ballooning instabilities, the analysis predicts the same behavior as in the high field. However, if the global equilibrium evolution is sufficiently slow, we speculate that enhanced transport across the mode would further slow the growth of Γ_0 and the system would exhibit a "soft" β limit as the system moves slowly through region II. For ballooning modes in magnetospheric plasmas the approach to the marginal stability boundary would occur during the "growth phase" of the substorm. Here, roughly, $\Delta \geq 1$ so a linear instability evolves directly to explosive singularity in approximately 800–1200 s. A plasma sheet configuration in region I may also be sufficiently excited by an external trigger to result in explosive instability on the same time scale.

This work was supported by the U.S. Department of Energy, the National Science Foundation, and the National Aeronautics and Space Administration.

*Permanent address: Princeton University Plasma Physics Laboratory, Princeton, NJ 08543-0451.

[1] E. D. Fredrickson *et al.*, Phys. Plasmas **3**, 2620 (1996).
[2] W. Park *et al.*, Phys. Rev. Lett. **75**, 1763 (1995).
[3] T. Gold, J. Geophys. Res. **64**, 1219 (1959).
[4] A. Roux *et al.*, J. Geophys. Res. **96**, 17 679 (1991).
[5] J. W. Connor, R. J. Hastie, and J. B. Taylor, Proc. R. Soc. London A **365**, 1 (1979); Y. C. Lee and J. W. Van Dam, in *Proceedings of the Finite Beta Theory Workshop, Varenna, Italy, 1977,* edited by B. Coppi and W. Sadowski (U.S. Department of Energy, Washington, D.C., 1979), p. 93.
[6] S. C. Cowley and M. Artun, Phys. Rep. **283**, 185 (1997).
[7] W. A. Newcomb, Phys. Fluids **4**, 391 (1961).
[8] E. N. Parker, Astrophys. J. **145**, 811 (1966).
[9] O. A. Hurricane, B. H. Fong, and S. C. Cowley, Phys. Plasmas **4**, 3565 (1997).
[10] R. B. White, *Theory of Tokamak Plasmas* (North-Holland Physics, Amsterdam, 1989), p. 129.
[11] W. M. Tang, R. L. Dewar, and J. Manickam, Nucl. Fusion **22**, 1079 (1982).
[12] B. H. Fong, S. C. Cowley, and O. A. Hurricane (to be published).
[13] C. C. Hegna and J. D. Callen, Phys. Fluids B **4**, 3031 (1992).